Appl. Phys. A 91, 663–666 (2008)
DOI: 10.1007/s00339-008-4502-6

**Applied Physics A**
**Materials Science & Processing**

JIN CHEN
WEIYI LU
YU QIAO✉

# Cleavage cracking across twin boundaries in free-standing silicon thin films

Department of Structural Engineering, University of California – San Diego, La Jolla, CA 92093-0085, USA

**Received: 8 January 2008/Accepted: 4 March 2008**
**Published online: 12 April 2008 • © Springer-Verlag 2008**

**ABSTRACT** Cleavage cracking across twin boundaries in free-standing silicon thin films is investigated in a microtensile fracture experiment. If the twist misorientation is relatively small, the crack front transmission can be quite smooth; otherwise the fracture surface may be either planar or broken down into parallel terrains. In all the cases, the local fracture resistance tends to increase.

**PACS** 62.20.-x; 68.35.bg; 68.35.Gy; 68.37.-d; 62.20.mm

## 1 Introduction

While twinning is most pronounced in hexagonal close-packed (HCP) crystals such as zinc and magnesium, in silicon, which is a face-centered cubic (FCC) material, as the external stress and the temperature are relatively low, it can be an important deformation mechanism [1–3]. It has been repeatedly observed that during nucleation of crystalline clusters and film growth of polycrystalline silicon a large number of twins can be generated [4]. The former is associated with chair and boat configurations of network atoms [5, 6], and the latter is caused by ledges along crystallographic planes [7]. Twins can have significant influences on mechanical properties of solids [8–13]. Unlike grain boundaries, twin boundaries are of regular lattice structures. They can act as obstacles to dislocation motion and thus increase the yield strength. However, for silicon, the influence of twinning on fracture, particularly in the lower shelf of brittle-to-ductile transition region, has been rarely investigated. Previous studies in this area were focused on the twinning-induced crack initiation [14–16]. After microcrack generation, the nature of interactions between twin boundaries and cracks is still quite inadequately understood.

In a FCC crystal, twinning usually occurs along energetically favorable (111)[112] systems. The cleavage surfaces are either (111) or (110) planes. While a small portion of cracks and twin boundaries may be parallel to each other, most of them are misoriented. As a cleavage crack bypasses a twin, its surface must be twisted and tilted. In fracture experiments on bicrystals [17, 18], it was noticed that in a heterogeneous material cleavage paths can be interrupted. For example, when a cleavage front encounters a high-angle grain boundary, its advance rate can be largely reduced [19]. When it transmits across the boundary, the crystalline plane in the grain ahead of the boundary would be cracked first at a number of breakthrough points, and the final fracture would occur only after the persistent grain boundary areas fail. As the crack is broken down into a number of sections, the concave parts would be left behind the verge of propagating front, increasing the local fracture toughness through the crack trapping effect [20]. Another mechanism of boundary toughening is related to the competition between the increase in crack growth driving force and the increase in local cleavage resistance, which would eventually lead to unstable crack behaviors [21]. Since the interruptions of crack propagation at a twin boundary and at a grain boundary can be somewhat similar, it is reasonable to argue that twin boundaries may also have a toughening effect, which is in agreement with the observation of crack arrest at twins (e.g. [22]).

Silicon films are widely used in microfabrication and semiconductor industries [23]. Usually, the film thickness is at the μm level. In order to analyze the material behaviors most relevant to engineering practice, we carry out experiments on thin-film samples, so that the plane stress condition as well as the surface effect on deformation are similar to that of microcomponents [24]. The analysis is focused on the behaviors of individual twins. The interaction among them is beyond the scope of the current study.

## 2 Experimental

The thin-film samples were obtained from a boron-doped polycrystalline silicon wafer. The initial wafer thickness was 10 mm, and the grain size was 15–20 mm. The grains contained visible twins. The lattice structure of each grain was determined through Laue X-ray back reflection, and the twin systems could be identified based on their relative orientations. In order to generate pre-cracks, the wafer was heated at 370 °C for 30 min and then partly immersed in cold water. A large number of random thermal cracks were produced, and many of them were arrested by twins. Six suitable crack tips were marked and cut off by electrical discharge machining (EDM). Their fracture surfaces were all along $\{0\bar{1}1\}$

✉ Fax: 858-822-2260, E-mail: yqiao@ucsd.edu

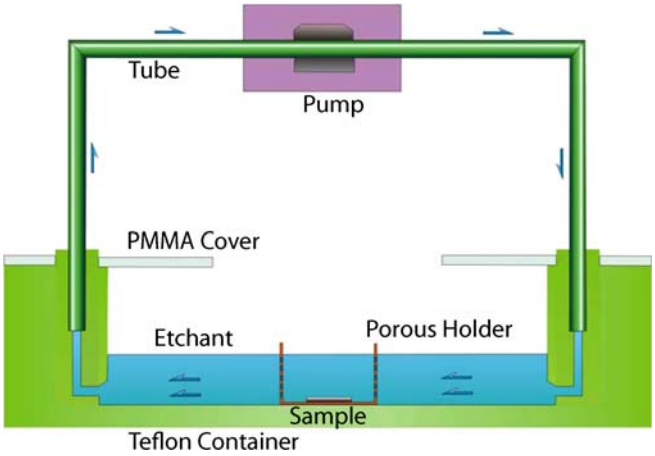


**FIGURE 1** Schematic of the etching system

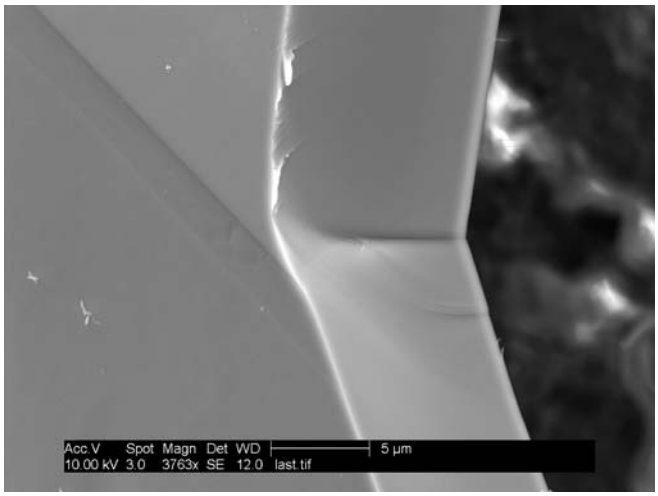


**FIGURE 2** A SEM image of the smooth transmission of a cleavage surface across a twin. The crack propagates from the top to the bottom

planes and the twin systems were $\{1\bar{1}1\}\langle\bar{1}12\rangle$; that is, they had the same crystalline orientation. The sectioned pieces, typically with the sizes of $10 \times 10 \times 10$ mm, were sliced by EDM into 150 to 200 μm thick films along the crack directions. The cutting path was parallel to the wafer surface. The silicon films were dried in a vacuum oven for 12 h and sealed in a vertical condenser by a drying tube with 100 ml of dry toluene. By using a thermal bath, the temperature was maintained at 95 °C. While stirring, 5 ml of chlorotrimethylsilane was dropped into the condenser. The system was refluxed for 5 days. Then, the films were taken out, washed by dry toluene and acetone, and dried in air. The film surfaces were slightly polished to expose the silicon phase. Through this treatment, the pre-crack surfaces were covered by a dense layer of silyl groups [25, 26]. In order to reduce the film thickness to the desired level, the silicon film was placed in a porous poly(methyl methacrylate) (PMMA) holder and immersed in an etchant (7% of hydrofluoric acid, 75% of nitric acid, and 18% of acetic acid) in a teflon container, as shown in Fig. 1. The etchant was driven by a tube pump at a constant rate of 3 ml/min. As it flowed across the sample surface, the sample was etched and the byproducts were carried away. The etching rate was in the range of 2–3 μm/min. The final film thickness was around 10–40 μm.

After being rinsed in acetone, the surface-modified thin film was mounted on the tension stage of a custom-designed microtesting machine [27, 28]. Through two compound-flexure loading frames [29], a tensile load normal to the pre-crack surface was applied, with the loading rate of 5 μm/min. The peak load, $P$, at which the pre-crack started to propagate unstably, was measured, based on which the effective fracture toughness was calculated as $K_{\mathrm{IC}} = P\sqrt{\pi a}\, f(a/w_0)$, where $a$ is the pre-crack length, $w$ is the sample width, and $f$ is a geometry factor taking account for the free-edge effect [30]. Figures 2–4 show typical SEM images of fracture surfaces.

## 3 Results and discussion

The critical stress intensity factors of the samples under investigation are 1.8 MPa $\mathrm{m}^{1/2}$ (sample 1), 2.1 MPa $\mathrm{m}^{1/2}$ (sample 2), 2.0 MPa $\mathrm{m}^{1/2}$ (sample 3), 2.1 MPa $\mathrm{m}^{1/2}$ (sample 4), 1.7 MPa $\mathrm{m}^{1/2}$ (sample 5), and 2.3 MPa $\mathrm{m}^{1/2}$ (sample 6), respectively, which are considerably higher than that of silicon single crystals (0.9–1 MPa $\mathrm{m}^{1/2}$) [31], indicating that twin boundaries are obstacles to cleavage cracking. It is interesting that, while the samples are of nominally the same cleavage plane and twin system, their failure modes are significantly different. In sample 1 (Fig. 2), the transmission of cleavage front across the twin boundaries is quite smooth. The film surface is parallel to the $\{100\}$ plane, and the film thickness is about 7 μm. The width of the twin is about 2 μm. When the cleavage front meets the first twin boundary, it continues on the $\{0\bar{1}1\}$ plane. Since the crystallographic misorientation of the twin is along the $\langle\bar{1}12\rangle$ direction, there are both twist and tilt angles between the fracture surfaces across the boundary, while the twist angle is relatively small. To shift to the new cleavage plane, the fracture surface rotates with respect to the crack propagation direction around a point near the film surface at the right-hand side. Around this point, secondary cracking occurs along the twin boundary, connecting the two fracture surfaces together. At the far end, close to the film surface at the left-hand side, the fracture surface is curved, transferring to the misoriented $\{0\bar{1}1\}$ plane quite smoothly, primarily due to the large number of available cleavage systems in silicon crystals [32]. The fracture surface remains wavy in the twin. At the second boundary, the crack front propagates without detectable interruptions. Unlike the first boundary, only a small fraction of the second one is exposed to the cleavage surface. After the crack bypasses the twin, the orientation of the fracture path is close to the $\{\bar{1}01\}$ plane, which has the smallest misorientation angles with the cleavage surface in the twin.

The thickness of sample 2 (Fig. 3a) is about 23 μm. The film surface is close to the $\{\bar{1}11\}$ plane. The twin thickness is around 4 μm. Different from sample 1, the fracture facets, both inside and outside the twin, are quite planar. When the crack front reaches the first twin boundary, it abruptly shifts to the $\{0\bar{1}1\}$ plane. This process is also depicted in Fig. 3b. There exists a transition point at the crack front, around which the cleavage plane turns by the required twist and tilt angles. Secondary cleavage takes place along the twin boundary so that the separation of the fracture flanks is completed. On the

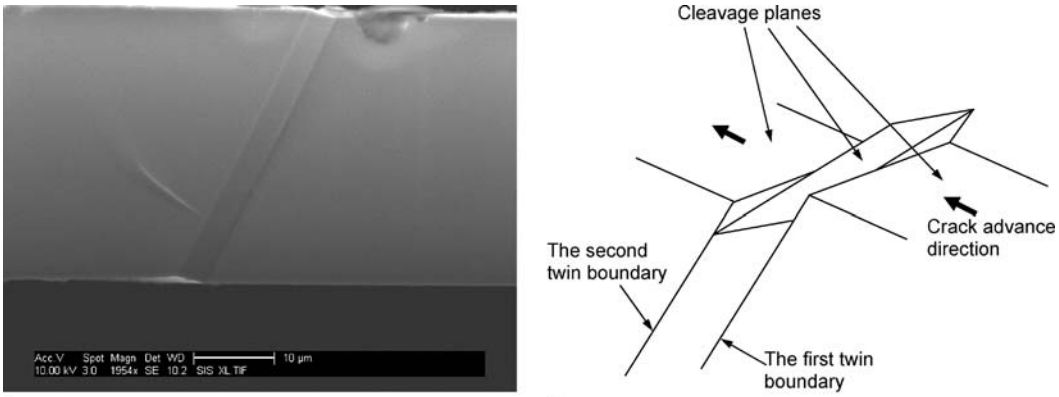


**FIGURE 3** (**a**) A SEM image and (**b**) a schematic diagram of the planar transmission of cleavage surface across a twin. The crack propagates from right to left

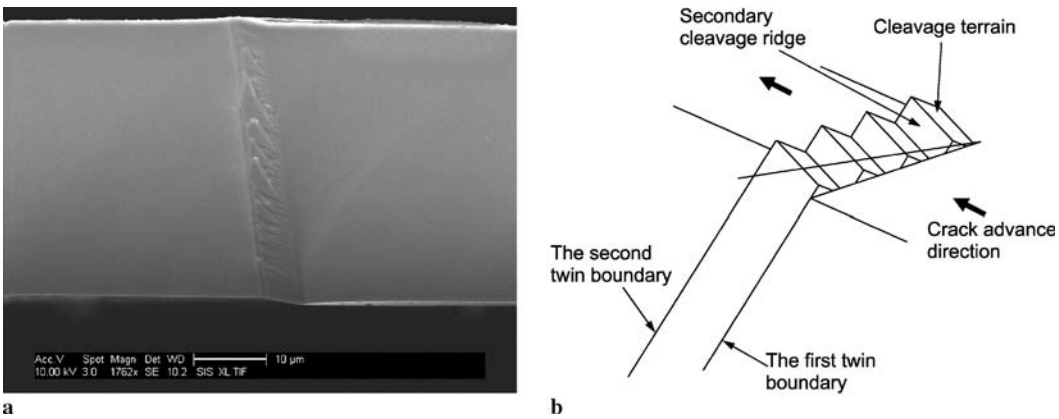


**FIGURE 4** (**a**) A SEM image and (**b**) a schematic diagram of sectioned transmission at the first twin boundary and recombination of cleavage facets at the second boundary. The crack propagates from right to left

SEM image, little river markings can be identified, suggesting that the front transmission occurs uniformly along the film thickness direction. The front keeps propagating to the second boundary and shifts back to the $\{0\bar{1}1\}$ plane, since it is of the most energetically favorable orientation under the applied loading. The fracture surfaces ahead of and behind the twins are parallel to each other, but have a height difference because of the tilt misorientation of the cleavage plane in the twin. Similar to the first boundary, secondary cracking takes place along the second boundary between the transmission point and the film surfaces.

Figure 4a shows that the thickness of sample 3 is about 32 μm. The crack propagates from right to left. The twin thickness is around 6 μm. The orientation of the film surface is near the $\{\bar{1}12\}$ plane. The cleavage plane in the twin is $\{011\}$. It is clear that the crack behavior is distinct from that of the first two samples. When the crack bypasses the first twin boundary, the fracture surface breaks down into a large number of terrains, which is depicted in Fig. 4b. Between adjacent terrains, secondary cracking happens along the cleavage planes normal to the primary cleavage surface, forming cleavage ridges, or river markings. The river markings are nearly parallel to each other, indicating that the cleavage front in the twin is quite straight, and thus the front transmission must occur almost simultaneously along the entire first twin boundary. The distance between the cleavage terrains is at the sub-μm level, ranging from 100 to 300 nm. At the second twin boundary, these terrains combine back into a single $\{0\bar{1}1\}$ plane, parallel to the fracture surface behind the first boundary.

The three types of crack front behaviors, namely the smooth transmission (Fig. 2), the planar transmission (Fig. 3), and the sectioned transmission (Fig. 4), represent all the crack-twin interaction modes in the samples under investigation. Since the twin system and the orientation of the cleavage plane are the same for each sample, it is likely that the difference in crack front behavior is caused by the twist misorientation of fracture surfaces across the first twin boundary. In the case of the smooth transmission, the twist angle is relatively small, and therefore by shifting among cleavage planes of similar orientations the crack front can overcome the barrier effect of the boundary. The associated fracture toughness, although much higher than that of crystallographic planes, is the lowest among all the modes. When the twist angles increase, there is a substantial gap between the fracture facets across the boundary. Under this condition, the smooth transmission becomes difficult and the planar transmission is dominant. Because the separation of twin boundaries demands additional work, the fracture resistance is higher than in the first case. As the twist angle rises further, if the crack front behavior were still in the planar transmission mode, the area of the twin boundaries involved in the process would be large. A more energetically favorable break-through mode is the sectioned transmission, in which the front transmits across

the first boundary at a number of break-through points and a series of parallel terrains are formed. Thus, the twin boundary area that must be fractured is largely reduced. However, the formation of cleavage ridges in the twin requires a certain amount of fracture work. Moreover, the persistent twin boundary areas in between the break-through points may have a crack trapping effect. Locally around a break-through point, the crack front profile can be curved, so the decrease in stress intensity at the crest of propagating front tends to increase the requirement of crack growth driving force. Consequently, if the number density of the terrains were too large the effective twin boundary fracture resistance would increase. The result of the two competing mechanisms leads to the regular river marking pattern observed in the experiment. Note that the crystals at both sides of the twin are of the same orientation. Hence, once the crack reaches the second twin boundary, the fracture surface tends to shift back to the original plane, so that the fracture work is minimized. That is, the front behaviors at the two twin boundaries are correlated.

The smooth crack front transmission shown in Fig. 2 may also be promoted by the relatively narrow twin width. Because the crystallographic orientation abruptly changes across the first twin boundary, the stress field ahead of the crack tip is distorted. If the second twin boundary is relatively far away from the first one, the distortion can be fully developed and mode I cracking is dominant. If the twin thickness is relatively small, the crack-tip stress field is constrained and the $T$-stress, i.e. the non-singular stress component, can be significant, which causes mode II cracking [33] and triggers the change in fracture direction. Additionally, the free surface effect on the stress field can be important, which explains why the cracking mode is different when the film surface orientation varies. If the film surface is close to the (100) plane, the distortion of the stress field along the transverse direction is relatively trivial, and thus the crack plane twisting is suppressed. Once the film surface deviates from this direction, the lattice structure in front of the crack front becomes asymmetric, and crystallographic planes of large twist misorientations tend to cleave. Furthermore, the front behavior should also be dependent on the film thickness. In a thin film, the integrity of the fracture surface is higher than that in a thick film. When the crack front is narrower, the front transmission tends to happen around a single break-through point; that is, the smooth or the planar transmission modes are easier. With increasing film thickness, the cleavage plane can be broken down into a few sections, resulting in the sectioned transmission mode.

## 4 Concluding remarks

Clearly, the above discussion does not provide a definitive answer to the question of what the dominant factors of crack-twin interactions are. Nevertheless, according to the experimental results, it can be seen that there are three main cleavage front transmission modes at twin boundaries. When the twist misorientation of cleavage planes across the first twin boundary is relatively small, the fracture surface tends to transmit smoothly into the twin. If the twist angle is relatively large, planar transmission mode dominates. As the twist misorientation further increases, the crack plane can break down into a number of terrains. After the crack front bypasses the second twin boundary, the fracture surface tends to be planar. In addition to the orientation of the crack plane and the twin system, the crack front transmission can also be associated with the effects of the orientation of the film surface, the film thickness, as well as the twin width. In all the cases, the fracture resistances offered by twin boundaries tends to be higher than that of single crystals.

## REFERENCES


1 M. Pitteri, G. Zanzotto, *Continuum Models for Phase Transitions and Twinning in Crystals* (CRC Press, Boca Raton, FL, 2002)
2 Y.Q. Wang, R. Smirani, G.G. Ross, Nano Lett. **4**, 2041 (2004)
3 Y.Q. Wang, R. Smirani, G.G. Ross, F. Schiettekatte, Phys. Rev. B **71**, 161 310 (2005)
4 R. Sinclair, J. Morgiel, A.S. Kirtikar, I.W. Wu, A. Chiang, Ultramicroscopy **51**, 41 (1993)
5 D. Pribat, P. Legagneux, F. Plais, C. Reita, F. Petinot, O. Huet, MRS Proc. **424**, 127 (1997)
6 R. Drosd, J. Washburn, J. Appl. Phys. **53**, 397 (1982)
7 F.A. McClintock, A.S. Argon, *Mechanical Behavior of Materials* (Ceramic Book & Literature Service, Marietta, OH, 1999)
8 L. Lu, M.L. Liu, K. Lu, Science **287**, 1463 (2000)
9 H.J. Song, X.H. Li, J.F. Huang, Chin. J. Chem. **24**, 273 (2006)
10 B.Q. Han, E.J. Lavernia, F.A. Mohamed, Rev. Adv. Mater. Sci. **9**, 1 (2005)
11 S.N. Gorin, L.M. Ivanova, Phys. Stat. Solidi B **202**, 221 (1997)
12 F. Hamdi, S. Asgari, Met. Mater. Trans. A **39A**, 294 (2008)
13 D.T.J. Hurle, P. Rudolph, J. Cryst. Growth **264**, 550 (2004)
14 A. Satta, E. Pisanu, L. Colombo, F. Cleri, J. Phys.: Condens. Matter **14**, 13 003 (2002)
15 P. Mullner, Solid State Phenom. **87**, 227 (2002)
16 G. Wagner, P. Paufler, Phys. Stat. Solidi A **113**, 389 (1993)
17 Y. Qiao, A.S. Argon, Mech. Mater. **35**, 129 (2003)
18 Y. Qiao, A.S. Argon, Mech. Mater. **35**, 313 (2003)
19 K. Ravi-Chandar, *Dynamic Fracture* (Elsevier Sci., San Diego, CA, 2004)
20 X. Kong, Y. Qiao, Fatigue Fract. Eng. Mater. Struct. **28**, 753 (2005)
21 Y. Qiao, Mater. Sci. Eng. A **361**, 350 (2003)
22 D. Hull, *Fractography* (Cambridge Univ. Press, Cambridge, UK, 1999)
23 M.J. Madou, *Fundamentals of Microfabrication* (CRC Press, Baco Raton, FL, 2002)
24 L.B. Freund, S. Suresh, *Thin Film Materials* (Cambridge Univ. Press, Cambridge, UK, 2004)
25 A. Han, Y. Qiao, Langmuir **23**, 11 396 (2007)
26 A. Han, Y. Qiao, Chem. Lett. **36**, 882 (2007)
27 A. Han, Y. Qiao, J. Phys. D Appl. Phys. **40**, 5743 (2007)
28 J. Chen, Y. Qiao, Scripta Mater. **57**, 1069 (2007)
29 J. Chen, Y. Qiao, Appl. Phys. A, in press
30 S. Gudlavalleti, L. Anand, in: Proc. 2001 ASME IMECE (New York, 2001)
31 B.L. Boyce, J. M Grazier, T.E. Buchheit, M.J. Shaw, J. MEMS **16**, 179 (2007)
32 D.H. Alsem, O.N. Pierron, E.A. Stach, C.L. Muhlstein, R.O. Ritchie, Adv. Eng. Mater. **9**, 15 (2007)
33 M.F. Kanninen, C.H. Popelar, *Advanced Fracture Mechanics* (Oxford Univ. Press, Oxford, UK, 1985)